

See discussions, stats, and author profiles for this publication at: <https://www.researchgate.net/publication/6386383>

# Direct Evidence of Arsenic(III)–Carbonate Complexes Obtained Using Electrochemical Scanning Tunneling Microscopy

ARTICLE *in* ANALYTICAL CHEMISTRY · JUNE 2007

Impact Factor: 5.64 · DOI: 10.1021/ac062244t · Source: PubMed

CITATIONS

12

READS

52

6 AUTHORS, INCLUDING:



Jumin Hao

Agiltron Inc.

28 PUBLICATIONS 410 CITATIONS

SEE PROFILE



Christos Christodoulatos

Stevens Institute of Technology

102 PUBLICATIONS 2,099 CITATIONS

SEE PROFILE



Xiaoguang Meng

Stevens Institute of Technology

83 PUBLICATIONS 3,560 CITATIONS

SEE PROFILE

# Direct Evidence of Arsenic(III)–Carbonate Complexes Obtained Using Electrochemical Scanning Tunneling Microscopy

Mei-Juan Han,<sup>†</sup> Jumin Hao,<sup>†</sup> Christos Christodoulatos,<sup>†</sup> George P. Korfiatis,<sup>†</sup> Li-Jun Wan,<sup>‡</sup> and Xiaoguang Meng<sup>\*,†</sup>

Center for Environmental Systems, Stevens Institute of Technology, Hoboken, New Jersey 07030, and Institute of Chemistry, Beijing National Laboratory for Molecular Sciences, Chinese Academy of Sciences (CAS), Beijing 100080, China

Electrochemical scanning tunneling microscopy (ECSTM), ion chromatography (IC), and electrospray ionization-mass spectrometry/mass spectrometry were applied to investigate the interactions between arsenite [As(III)] and carbonate and arsenate [As(V)] and carbonate. The chemical species in the single and binary component solutions of As(III), As(V), and carbonate were attached to a Au(111) surface and then imaged in a 0.1 M NaClO<sub>4</sub> solution at the molecular level by ECSTM. The molecules formed highly ordered adlayers on the Au(111) surface. High-resolution STM images revealed the orientation and packing arrangement of the molecular adlayers. Matching the STM images with the molecular models constructed using the Hyperchem software package indicated that As(III) formed two types of complexes with carbonate, including As(OH)<sub>2</sub>CO<sub>3</sub><sup>−</sup> and As(OH)<sub>3</sub>(HCO<sub>3</sub><sup>−</sup>)<sub>2</sub>. No complexes were formed between As(V) and carbonate. IC chromatograms of the solutions revealed the emergence of the new peak only in the aged As(III)–carbonate solution. MS spectra showed the presence of a new peak at *m/z* 187 in the aged As(III)–carbonate solution. The results obtained with the three independent methods confirmed the formation of As(OH)<sub>2</sub>CO<sub>3</sub><sup>−</sup>. The results also indicated that As(OH)<sub>3</sub> could be associated with HCO<sub>3</sub><sup>−</sup> through a hydrogen bond. The knowledge of the formation of the As(III) and carbonate complexes will improve the understanding of As(III) mobility in the environment and removal of As(III) in water treatment systems.

Arsenic is a common contaminant in groundwater worldwide. Long-term exposure to arsenic can cause skin, lung, urinary bladder, liver, and kidney cancer in humans.<sup>1–5</sup> The most common

arsenic species in natural water and sediment are As(III) and As(V).<sup>6</sup> As(III) is more toxic to humans and has higher mobility in the environment than As(V). The mobility of the arsenic species and their adsorption by metal oxides and hydroxides are influenced by common anions such as phosphate, silicate, and carbonate.<sup>7,8</sup> This effect is usually attributed to competitive adsorption of the anions and arsenic species on the solid surface.

Recently, Kim et al.<sup>9</sup> and Lee and Nriagu<sup>10</sup> proposed the formation of As(III)–carbonate complexes, which increases the mobility of arsenic in groundwater aquifers. Neuberger and Helz<sup>11</sup> confirmed this hypothesis by measuring the solubility of As<sub>2</sub>O<sub>3</sub> in concentrated carbonate solutions. However, quantum chemical calculations indicate that As(III) carbonate complexes predicted from the lanthanide correlation are very unstable relative to arsenious acid H<sub>3</sub>AsO<sub>3</sub>.<sup>12</sup> Since carbonate is the most abundant anion in groundwater and surface water, further studies are necessary to determine the interactions between As(III) and carbonate.

The invention of scanning tunneling microscopy (STM) in the early 1980s<sup>13–15</sup> enabled imaging of chemical species at molecular and atomic resolution. STM is a surface analysis technique that probes the electronic properties of surfaces.<sup>16</sup> It can provide atomic resolution micrographs of individual molecules deposited on a solid surface in solution.<sup>17</sup> STM has been used to distinguish chiral molecules<sup>18–19</sup> and investigate the reaction mechanisms of

\* To whom correspondence should be addressed. E-mail: xmeng@stevens.edu.

<sup>†</sup> Stevens Institute of Technology.

<sup>‡</sup> Beijing National Laboratory for Molecular Sciences.

(1) Cullen, W. R.; Reimar, K. J. *Chem. Rev.* **1989**, 89, 713.

(2) WHO. *Arsenic, Environmental Health Criteria 18*; World Health Organization: Geneva, 1983.

(3) *Evaluation of Carcinogenic Risks to Humans, Overall Evaluations of Carcinogenicity: An Updating of IARC Monographs, Vols. 1–42*; Volume Supplement 7; International Agency for Research on Cancer: Lyon, 1987; p 100.

(4) Wu, M. M.; Kuo, T. L.; Hwang, Y. H.; Chen, C. J. *Am. J. Epidemiol.* **1989**, 130, 1123.

(5) Bates, M. N.; Smith, A. H.; Hopenhayn-Rich, C. *Am. J. Epidemiol.* **1992**, 135, 462.

(6) Smith, A. H.; Hopenhayn-Rich, C.; Bates, M. N.; Goeden, H. M.; Hertz, Picciotto, I.; Duggan, H. M.; Wood, R.; Kosnett, M. J.; Smith, M. T. *Environ. Health Perspect.* **1992**, 97, 259.

(7) Meng, X.; Bang, S.; Korfiatis, G. P. *Water Res.* **2000**, 34, 1255.

(8) Meng, X. G.; Korfiatis, G. P.; Christodoulatos, C.; Bang, S. B. *Water Res.* **2001**, 35, 2805.

(9) Kim, M.-J.; Nriagu, J.; Haack, S. *Environ. Sci. Technol.* **2000**, 34, 3094.

(10) Lee, J. S.; Nriagu, J. O. *Am. Chem. Soc., Symp. Ser.* **2003**, 835, 33.

(11) Neuberger, C. S.; Helz, G. R. *Appl. Geochem.* **2005**, 20, 1218.

(12) Tossell, J. A. *Am. Chem. Soc., Symp. Ser.* **2004**, 915, 118.

(13) Binnig, G.; Rohrer, H. *Helv. Phys. Acta* **1982**, 55, 726.

(14) Binnig, G.; Rohrer, H.; Gerber, Ch.; Weibel, E. *Appl. Phys. Lett.* **1982**, 40, 178.

(15) Binnig, G.; Rohrer, H.; Gerber, Ch.; Weibel, E. *Phys. Rev. Lett.* **1982**, 49, 57.

(16) Wiesendanger, R.; Bode, M.; Dombrowski, R.; Getzlaff, M.; Morgenstern, M.; Wittneven, C. *Jpn. J. Appl. Phys.* **1998**, 37, 3769.

(17) Weiss, P. S.; Eigler, D. M. *Phys. Rev. Lett.* **1993**, 71, 3139.

(18) Xu, Q. M.; Wang, D.; Wan, L. J.; Wang, C.; Bai, C. L.; Feng, G. Q.; Wang, M. X. *Angew. Chem., Int. Ed.* **2002**, 41, 3408.

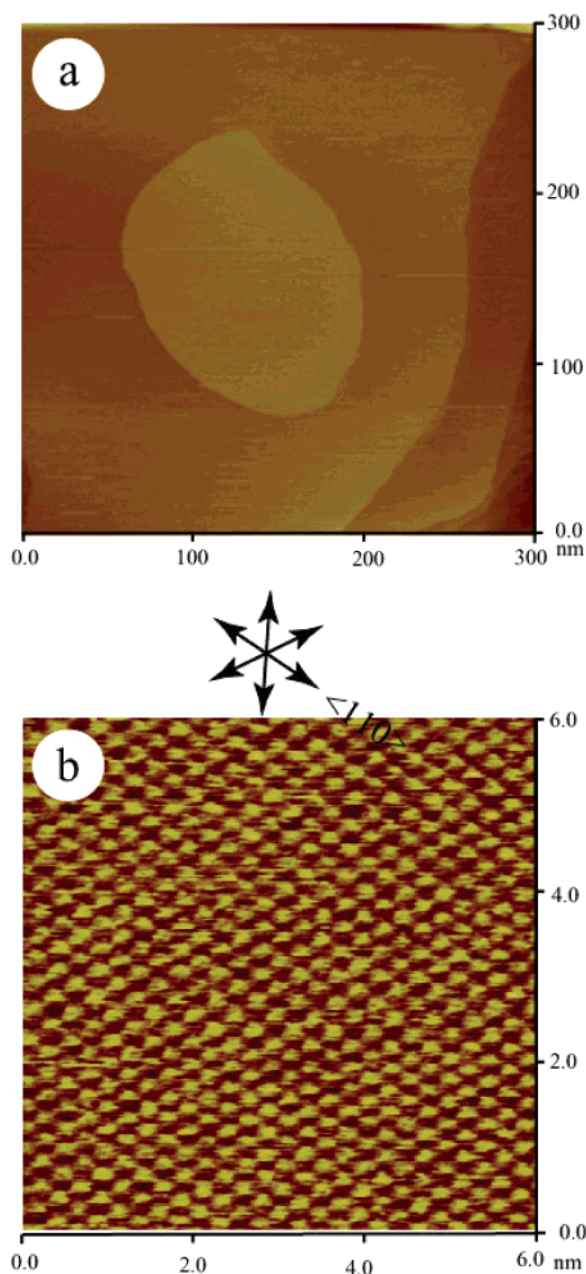


**Figure 1.** STM top view of Au(111) in 0.1 M NaClO<sub>4</sub>. (a) Large-scale STM image obtained at 0.4 V showing a clean, atomically flat Au(111) surface. Tunneling current was 1.0 nA. (b) Au(111)-(1 × 1) structure obtained at 0.6 V. Tunneling current was 2.0 nA.

catalytic oxidation of hydrogen on a platinum surface<sup>20</sup> and carbon monoxide on a rhodium surface.<sup>21</sup>

In the present study, electrochemical scanning tunneling microscopy (ECSTM), ion chromatography (IC), and electrospray ionization-mass spectrometry/mass spectrometry (ESI-MS/MS) were applied to investigate the interactions among As(III), As(V), and carbonate. In the ECSTM measurement, a sample is probed in an electrochemical cell containing solutions. Molecular

(19) Han, M.-J.; Wang, D.; Hao, J.-M.; Wan, L.-J.; Zeng, Q. D.; Fan, Q. H.; Bai, C. L. *Anal. Chem.* **2004**, *76*, 627.

(20) Völkening, S.; Bedürftig, K.; Jacobi, K.; Winterlin, J.; Ertl, G. *Phys. Rev. Lett.* **1999**, *83*, 2672.

(21) Cudia, C. C.; Hla, S. W.; Comelli, G.; Šljivančanin, Ž.; Hammer, B.; Baraldi, A.; Prince, K. C.; Rosei, R. *Phys. Rev. Lett.* **2001**, *87*, 196104-1.

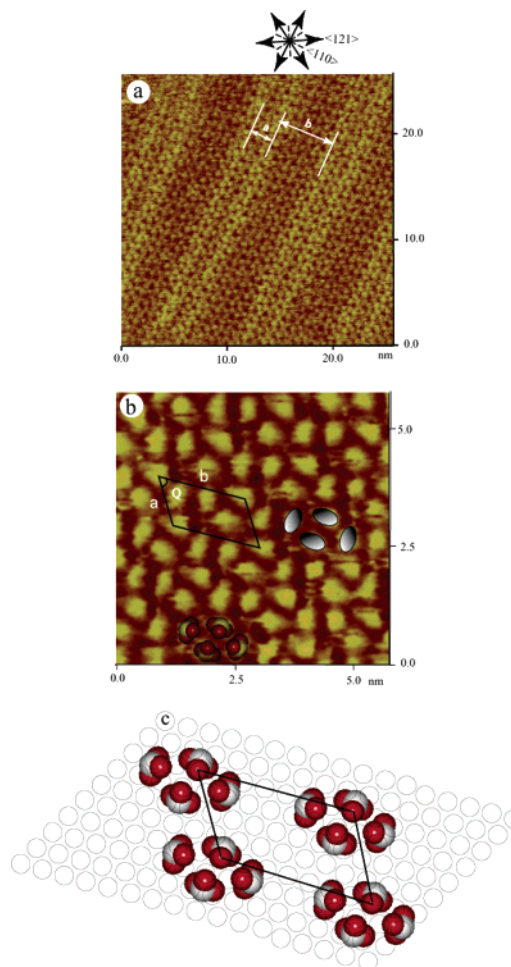


**Figure 2.** (a) Large-scale STM image of As(III) adlayer on Au(111) surface acquired at 0.6 V. Tunneling current was 2.0 nA. (b) High-resolution STM image of As(III) adlattice. Tunneling current was 2.0 nA. (c) A proposed model for the As(III) adlayer.

models of the individual arsenic and carbonate species and their potential complexes were constructed using the Hyperchem software package. The models were compared with the STM images to determine the complexes formed in the systems. In order to further verify the presence of the complexes, the solution samples were also analyzed using IC and MS. The results provide direct evidence of the formation of arsenic–carbonate complexes, which are important for predicting the environmental mobility of arsenic and the development of effective water treatment systems for arsenic removal.

## EXPERIMENTAL SECTION

**Chemicals.** A solution of 0.1 M NaClO<sub>4</sub> was prepared by dissolving NaClO<sub>4</sub> (Fisher Scientific, HPLC grade) into Milli-Q water (18.2 MΩ and TOC <5 ppb). Arsenic and carbonate solutions (0.1 mM) were prepared with reagent grade or certified ACS grade chemicals of sodium arsenite, sodium hydrogen arsenate, and sodium carbonate (Fisher Scientific), respectively. The binary component solutions of As(III)–carbonate and As(V)–carbonate were prepared by mixing equal volumes of arsenic and carbonate solutions. The mixed solutions were aged for 24 h under N<sub>2</sub> in order to ensure complete reactions among the arsenic species and carbonate.



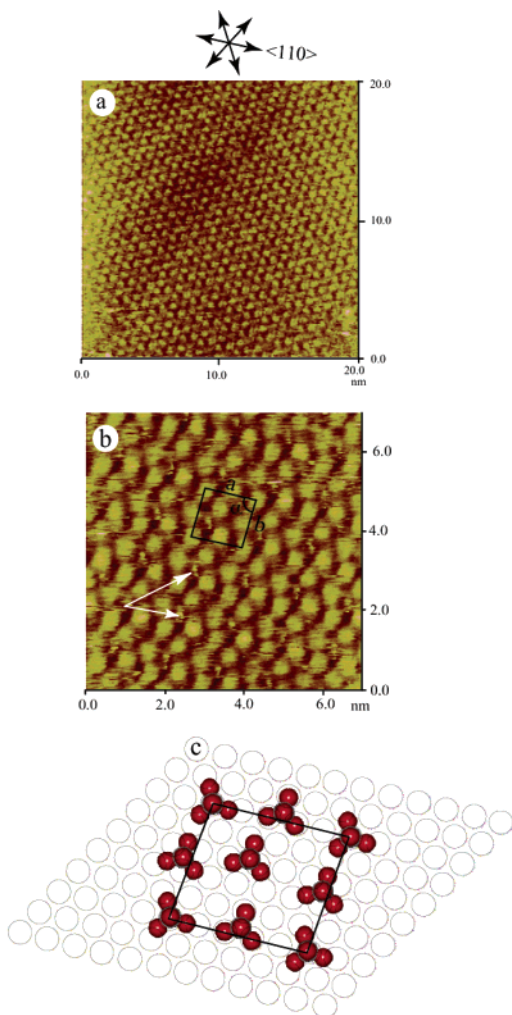


**Figure 3.** (a) STM image of As(V) molecules on Au(111) surface in 0.1 M NaClO<sub>4</sub> at 0.6 V. Tunneling current was 2.0 nA. (b) High-resolution STM image of As(V) array on Au(111) surface in 0.1 M NaClO<sub>4</sub> at 0.6 V. Tunneling current was 2.0 nA. (c) Schematic representation for the  $(5 \times \sqrt{19})$  structure.

**Preparation of STM Substrate.** A well-defined Au(111) electrode was prepared by crystallization of a molten ball formed at the end of a Au wire (99.999%) in a hydrogen–oxygen flame and was used as the substrate for the STM experiments.<sup>22–24</sup> Before each measurement, the Au(111) electrode was further annealed in a hydrogen–oxygen flame and quenched in ultrapure water (Milli-Q) saturated with hydrogen to obtain a clean  $(1 \times 1)$  structure.

**STM Measurements.** Molecular adlayers were prepared on the Au(111) surface by immersing the single-crystal gold bead into solutions containing 0.1 mM As(III), As(V), carbonate, and their mixtures for 1 min. Then, the Au(111) electrode was rinsed with Milli-Q ultrapure water to remove the residual molecules and transferred into the STM electrochemical cell. The STM experiments were performed in 0.1 M NaClO<sub>4</sub> solution to prevent the contamination of the gold surface in an open atmosphere.<sup>22,23</sup>

Electrochemical STM measurements were carried out with a Nanoscope IIIa microscope (Digital Instrument Inc.) under

potential control in the double-layer potential region. The reference and counter electrodes were platinum wires, and all potentials are reported with respect to the reversible hydrogen electrode in 0.1 M NaClO<sub>4</sub>. The STM tips were prepared by electrochemically etching (12–15 V) a tungsten wire (0.25 mm in diameter) in 0.6 M KOH until the etching process stopped. The tungsten tips were coated with clear nail polish to minimize faradic current. All images were acquired in the constant-current mode to evaluate the corrugation heights of the Au(111) substrate and the adsorbed molecules. All molecular models were constructed and optimized using the Hyperchem software package (version 6.0).

**IC and ESI-MS Analyses.** Single As(III) (25 mM), As(V) (2.5 mM), and carbonate (25 mM) solutions were prepared. The binary component solution (25 mM) of As(III)–carbonate was prepared by mixing equal volumes As(III) and carbonate solutions. Both fresh and aged (24 h under N<sub>2</sub>) binary solutions were prepared. The chemical species in the single and mixed solutions were detected using IC (Dionex) equipped with AS14 analytical anion-exchange column and a 25-μL sample loop. A 1 mM NaHCO<sub>3</sub> and 1 mM Na<sub>2</sub>CO<sub>3</sub> (pH = 8.8) solution was used as mobile phase at a flow rate of 1.0 mL/min. The mobile-phase solution was degassed by N<sub>2</sub> for 30 min before IC analysis.

Aged binary solution (1.0 mM) of As(III)–carbonate was analyzed using ESI-MS/MS on a Micromass Quattro 1 spectrometer equipped with an electrospray source. Samples were introduced into the spectrometer using a syringe pump.

## RESULTS AND DISCUSSION

**Arsenic Monomolecular Adlayer and Structure Characteristics.** The atomic image of the Au(111)- $(1 \times 1)$  structure was discerned on clean and atomically flat Au(111) terraces in 0.1 M NaClO<sub>4</sub> before each experiment in order to determine the orientation of the molecular adlayer with respect to the underlying Au(111) lattice. A clean and atomically flat Au(111) surface with a well-defined terrace-step structure was produced following the method described in the literatures.<sup>25,26</sup> Figure 1a is a typical large-scale STM image of a clean Au(111) surface. The terraces are mostly more than 100 nm wide. Figure 1b shows a high-resolution STM image obtained on an atomically flat terrace. Each bright spot represents a gold atom. The Au(111) surface shows a well-ordered hexagonal close-packed structure, as indicated by the arrows in Figure 1b. The observed nearest-neighbor atomic spacing is  $0.288 \pm 0.05$  nm, which is in excellent agreement with the lattice constant value (0.289 nm) for the Au(111) surface.<sup>26</sup> The images indicated that the Au(111) surface was clean and had a well-ordered  $(1 \times 1)$  structure.

The adlayer structure of As(III) was observed sequentially by STM in 0.1 M NaClO<sub>4</sub> solution. The atomically flat terraces were now covered with an ordered As(III) adlayer. Figure 2a is a large-scale STM image of the As(III) adlayer. This image was acquired at 0.6 V in 0.1 M NaClO<sub>4</sub>. The self-assembled monolayer consisted of molecular rows and extended over the flat terrace of the substrate surface. Molecular defects existed in the domain boundaries. The results directly demonstrated that a self-assembled monolayer of As(III) was successfully prepared on the Au(111) surface.

(22) Xu, S.; Szymanski, G.; Lipkowski, J. *J. Am. Chem. Soc.* **2004**, *126*, 12276.

(23) Yoshimoto, S.; Suto, K.; Tada, A.; Kobayashi, N.; Itaya, K. *J. Am. Chem. Soc.* **2004**, *126*, 8020.

(24) Yoshimoto, S.; Higa, N.; Itaya, K. *J. Am. Chem. Soc.* **2004**, *126*, 8540.

(25) Kunitake, M.; Akiba, U.; Batina, N.; Itaya, K. *Langmuir* **1997**, *13*, 1607.

(26) Wan, L.-J.; Terashima, M.; Noda, H.; Osawa, M. *J. Phys. Chem. B* **2000**, *104*, 3563.

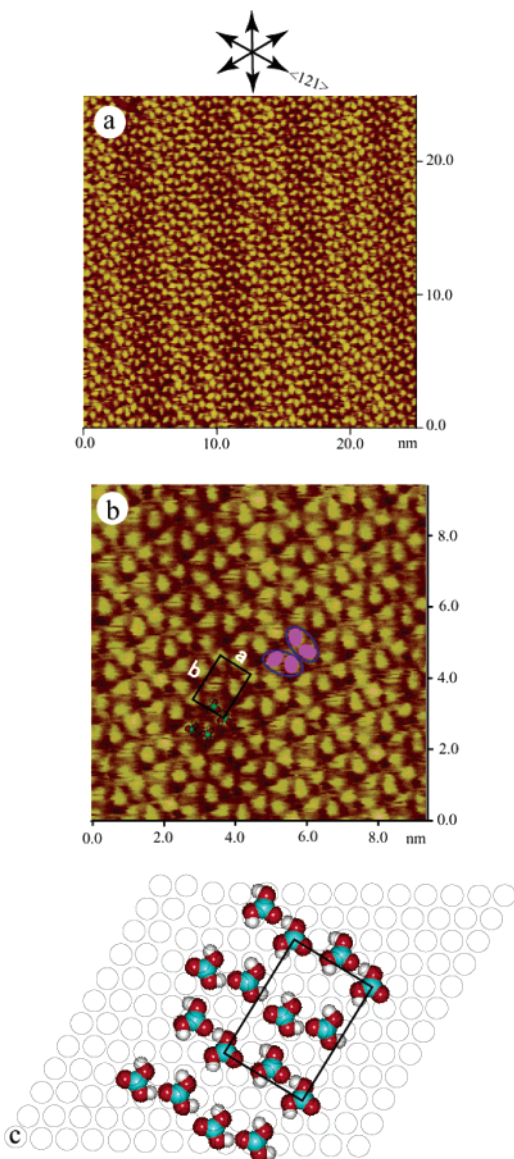


**Figure 4.** (a) STM image of carbonate molecules on Au(111) surface in 0.1 M NaClO<sub>4</sub> at 0.6 V. Tunneling current was 2.0 nA. (b) High-resolution STM image of carbonate array on Au(111) surface in 0.1 M NaClO<sub>4</sub> at 0.6 V. Tunneling current was 2.0 nA. (c) Schematic representation for the  $(5 \times 2\sqrt{3})$  structure.

The bright stripes seen in Figure 2a are the herringbone reconstruction rows of the underlying Au(111) surface. The Au(111)- $(23 \times \sqrt{3})$  reconstruction was evidenced by herringbone patterns with conspicuous pairs of stripes.<sup>27–28</sup> The distance between stripes was  $\sim 2.80$  nm (denoted by letter “a” in Figure 2a) and that between pairs was  $\sim 6.14$  nm (indicated by letter “b” in Figure 2a), which is consistent with the result obtained on bare Au(111) both in UHV<sup>27</sup> and in air.<sup>28</sup> The Au(111)- $(23 \times \sqrt{3})$  reconstruction is characterized by a 4.2% uniaxial lateral contraction of the surface layer along the  $\langle 110 \rangle$  direction, which is perpendicular to the herringbone rows.<sup>27</sup> The surface structures are used to establish the crystallographic orientation of the substrate.<sup>29</sup>

(27) Esplandiú, M. J.; Hagenström, H.; Kolb, D. M. *Langmuir* **2001**, *17*, 828.  
(28) Wöll, Ch.; Chiang, S.; Wilson, R. J.; Lippel, P. H. *Phys. Rev. B* **1989**, *39*, 7988.

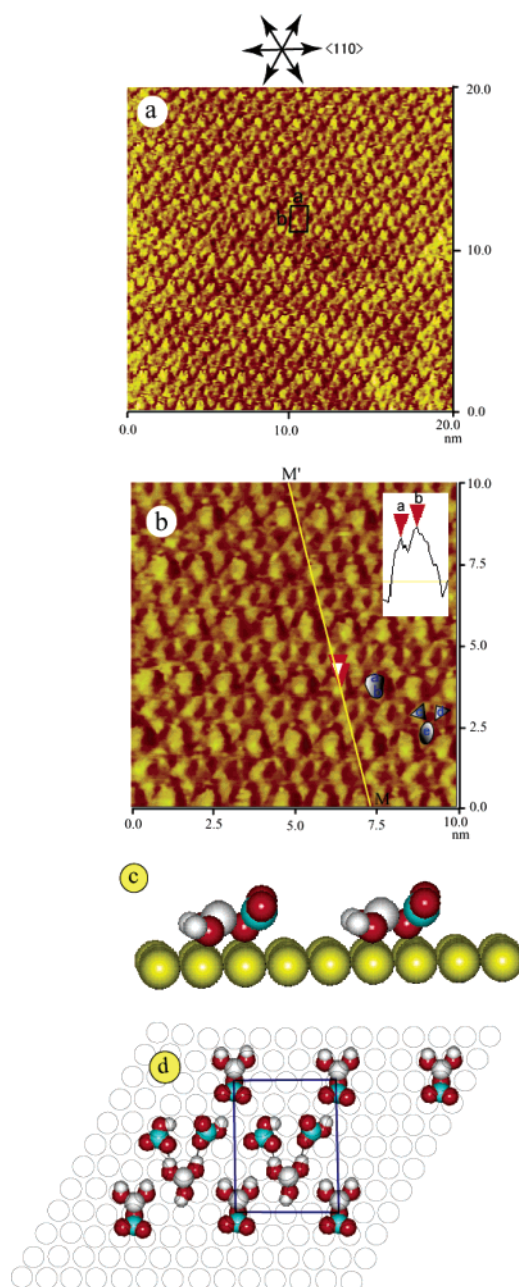


**Figure 5.** (a) Large-scale STM image of complex adlayer on Au(111) surface acquired at 0.6 V. Tunneling current was 2.0 nA. (b) High-resolution STM image of complex adlayer. Tunneling current was 2.0 nA. (c) Side view of As(OH)<sub>2</sub>CO<sub>3</sub><sup>−</sup> adsorbed on Au(111) surface. (d) A proposed model for the complex adlayer.

Figure 2b is a typical higher resolution STM image acquired on an As(III) adlayer at 0.6 V. The structural details of the ordered adlayer can be seen clearly from this higher resolution STM image. Each repeat unit has four bright spots in a molecular row. This interesting feature is outlined by four oval rings in Figure 2b. From the chemical structure and dimensions of As(III), it is clear that each spot in the repeat unit corresponds to an As(III) molecule. A schematic illustration for this molecular arrangement is shown in Figure 2b. The repeat distances along the *a* and *b* directions were measured to be 1.2 and 2.0 nm, respectively, with

(29) Doderio, G.; De Micheli, L.; Cavalleri, O.; Rolandi, R.; Oliveri, L.; Daccà, A.; Parpdi, R. *Colloids Surf. A* **2000**, *175*, 121.



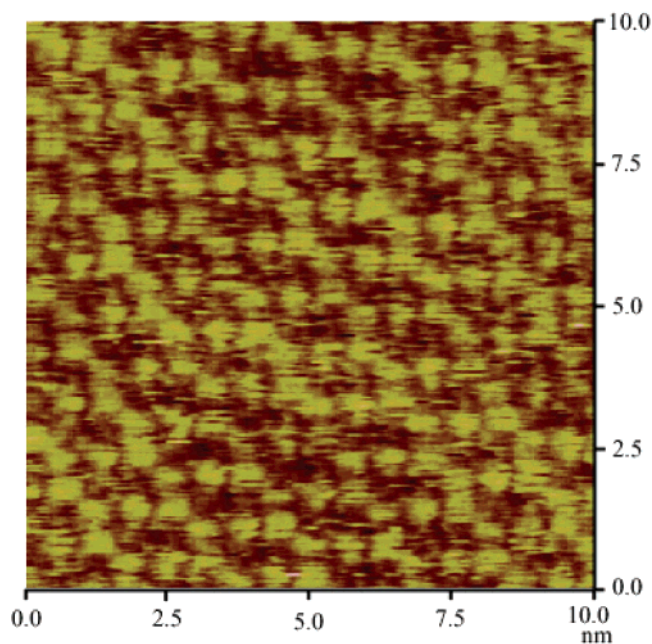


**Figure 6.** STM image for fresh As(III)-carbonate solution. The image was obtained in 0.1 M NaClO<sub>4</sub> at 0.6 V.

an experimental error of  $\pm 0.2$  nm. The internal angle  $Q$  between  $a$  and  $b$  was  $59 \pm 2^\circ$ . The molecular rows are along the close-packed directions of the Au(111) lattice by comparison with the underlying substrate Au(111)-(1  $\times$  1). On the basis of the orientation of molecular rows and the intermolecular distance, we conclude that the observed adlayer possesses a (4  $\times$  7) structure. A unit cell is outlined in Figure 2b. In view of the space in a repeat unit, it is impossible for As(III) molecules lying on the surface to have three oxygen atoms interacting with the gold substrate. Thus, the As(III) molecules may be in a vertical (tilted) orientation on the surface. Based on the above analysis, a structural model is proposed in Figure 2c. This result is different from that reported by Feliu.<sup>30</sup> Fourier transform infrared spectroscopy, cyclic voltammograms, and an ex situ STM study of irreversibly adsorbed As(III) on Pt(111) has been performed in different test solutions. They found the arsenic formed a ( $\sqrt{3} \times \sqrt{3}$ ) adlayer on Pt(111) surface in air. From previous studies,<sup>31–33</sup> it was found that different adlayer structures for the same molecule could be observed on different metal substrates, and the same adlayer structures for different molecules could be formed on the same metal substrate.

The above image processing procedures were also applied for all the other systems in this paper. Figure 3a shows a typical large-scale STM image of As(V) adlayer acquired at 0.6 V in a 20-nm<sup>2</sup> area. Although As(V) molecules also form large and uniform molecular arrays, it is obvious that the adsorption style of the As(V) is different from that of the As(III). The repeat distances along the  $a$  and  $b$  directions were 1.4 and 1.2 nm, respectively, with an experimental error of  $\pm 0.2$  nm. The internal angle  $\alpha$  between  $a$  and  $b$  was  $85 \pm 2^\circ$  and a (5  $\times$   $\sqrt{19}$ ) structure was deduced. From

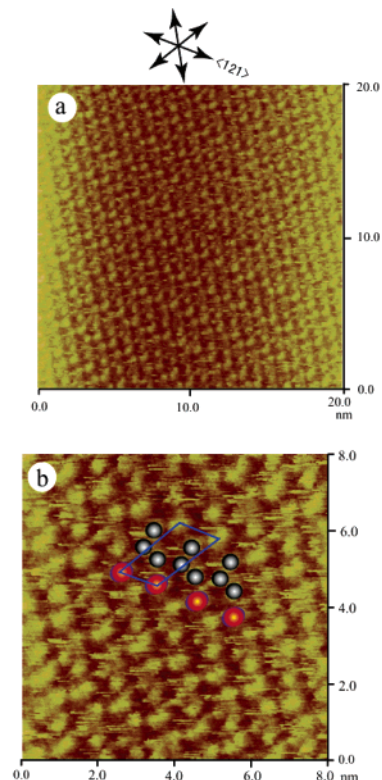


**Figure 7.** (a) STM image of molecules in As(V)-carbonate system on Au(111) surface in 0.1 M NaClO<sub>4</sub> at 0.6 V. (b) Higher resolution STM image of this system array on Au(111) surface in 0.1 M NaClO<sub>4</sub> at 0.6 V. (c) Schematic representation for the (2 $\sqrt{3}$   $\times$  4 $\sqrt{3}$ ) structure.

the higher resolution image in Figure 3b, some small spots denoted by arrows can be seen. They may be ascribed to hydronium ions, water molecules, or both. A unit cell is outlined in Figure 3b. Figure 3c shows a structural model of the As(V) adsorption on Au(111).

The molecular appearance in STM images depends on the chemical structure of the molecule, the crystallography of the underlying substrate, and the interactions between the molecules and between the molecule and substrate. The formation of the four-bright-spots structure in Figure 2b could be attributed to intermolecular interactions between As(III) molecules, which are stronger than the interactions between As(III) and the Au atoms. The relatively uniform distribution of the As(V) molecules on the Au surface may suggest that the strength of intermolecular interactions between the As(V) molecules and between As(V) and the Au atoms are similar.

**Carbonate Monomolecular Adlayer and Its Structure Characteristics.** Figure 4 illustrates that carbonate formed a highly ordered monolayer on the Au(111) surface. From the typical large-scale STM image (Figure 4a) obtained at 0.60 V with

(30) Orts, J. M.; Rods, A.; Feliu, J. M. *J. Electroanal. Chem.* **1997**, *434*, 121.

(31) Yau, S.-L.; Kim, Y.-G.; Itaya, K. *J. Phys. Chem. B* **1997**, *101*, 3547.

(32) Wan, L. J.; Itaya, K. *Langmuir* **1997**, *13*, 7173.

(33) Shimooka, T.; Yoshimoto, S.; Wakisaka, M.; Inukai, J.; Itaya, K. *Langmuir* **2001**, *17*, 6380.

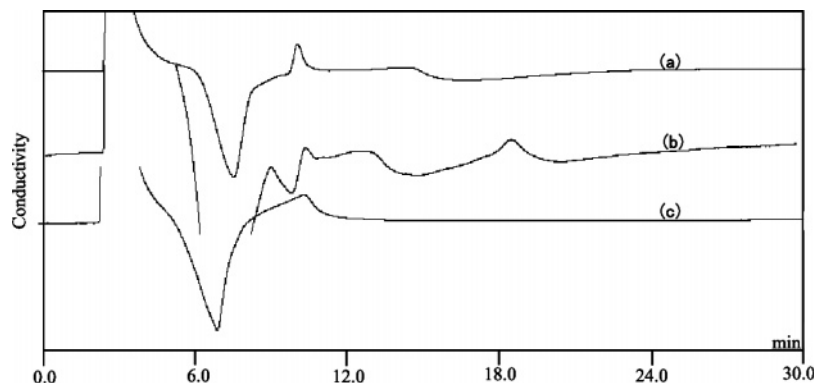


**Figure 8.** IC chromatograms for (a) single arsenite solution, (b) aged As(III)–carbonate solution, and (c) fresh As(III)–carbonate solution.

a bias voltage of  $-211$  mV and a set-point current of  $2.0$  nA, it can be seen that carbonate molecules form a long-range adlayer. The high-resolution STM image (Figure 4b) revealed that the carbonate adlayer consists of molecular clusters. Each cluster outlined by two ellipses (blue) can be recognized to contain two oval rings (purple) composed of two spots in the STM image (shown in Figure 4b). By comparison with the chemical structure of the carbonate molecule, each oval ring (purple) shape is assumed to be a molecule. Previous literature has described that the carbonate formed rods on the Ag(110) surface, appearing as a disordered formation.<sup>34</sup> This is also caused from the different metal substrates.<sup>31–33</sup>

The two molecular rows of carbonate, denoted by arrows *a* and *b*, are rotated  $\sim 90^\circ$  with respect to each other. In comparison with the underlying Au(111) lattice, the molecular rows *a* are parallel to the  $\langle 121 \rangle$  direction while the molecular rows *b* are parallel to the  $\langle 110 \rangle$  direction. The repeat distances along the *a* and *b* directions are  $1.0 \pm 0.2$  and  $1.4 \pm 0.1$  nm, respectively. According to the atom arrangement of the Au(111) surface, a unit cell with  $(5 \times 2\sqrt{3})$  symmetry is outlined in Figure 4b. Based on the above analysis, a model (shown in Figure 4c) can be constructed for the ordered array of carbonate.

**Interactions among Arsenic and Carbonate Species in the Mixed Solutions.** The molecules in the binary solutions of As(III)–carbonate and As(V)–carbonate were deposited on the Au(111) surface and imaged to determine whether the arsenic species formed complexes with carbonate. Figure 5a is a large-scale STM image of the adlayer for the aged As(III)–carbonate system. The intermolecular distance was  $\sim 1.16$  nm along the direction *a*. The intermolecular distance along the direction *b* was  $\sim 1.58$  nm. The internal angle between *a* and *b* is  $\sim 90^\circ$ . Therefore, the adlayer of the complex can be assigned to a  $(4 \times 3\sqrt{3})$  structure by comparison with the Au(111) substrate. A unit cell is outlined in Figure 5a and contains two complex molecules.

The features of the molecules for the As(III)–carbonate system can be clearly seen from the high-resolution STM image shown in Figure 5b. The appearance of the adlayer was completely different from those of As(III) in Figure 2 and carbonate in Figure 4, although similar STM imaging conditions were used in acquiring the images. Figure 5b shows the presence of two differently shaped species: (a) large elongated spots represented by a rough circle and (b) triple-spot combinations labeled with a

rough circle topped with two triangles. Since the sizes of the two species are larger than individual As(III) and carbonate, they could represent complexes formed between As(III) and carbonate. The elongated spot is measured to be  $\sim 0.7$  nm in the MM' direction, compared to the sizes of As(III) ( $\sim 0.5$  nm) and carbonate ( $\sim 0.4$  nm).

It has been reported that carbonate and As(III) can form carbonate complexes, such as  $\text{As}(\text{CO}_3)^+$ ,  $\text{As}(\text{CO}_3)_2^-$ , and  $\text{As}(\text{OH})_2\text{CO}_3^-$ .<sup>9–10</sup> Among them,  $\text{As}(\text{OH})_2\text{CO}_3^-$  is believed to be the most stable complex.<sup>11</sup> Based on the configuration of  $\text{As}(\text{OH})_2\text{CO}_3^-$  constructed with the Hyperchem software, the length of the complex is  $0.64$  nm. Therefore, it is reasonable to attribute the elongated spot to  $\text{As}(\text{OH})_2\text{CO}_3^-$ . The arsenic is associated with carbon through As–O–C bonds. A close examination revealed that each elongated spot consisted of two bright spots as labeled (a) and (b) in Figure 5b. The spot marked (b) is smaller in size than that marked (a), while more intense in brightness. The inset in the top-right corner shows a cross-sectional profile of the complex along the MM' direction. It is clearly seen that there is a difference in corrugation height in the intramolecule. On the basis of these results, we deduced that the three oxygen atoms, which are directly associated with the As atom, bind to the Au(111) surface. The other two oxygen atoms associated with carbon protrude from the surface, resulting in a height difference. Figure 5c is a side view of the proposed surface structure. Based on these analytic results and STM observations, the reasonable structure of the complex is tentatively depicted in the top and bottom rows in Figure 5d.

The three spots in the triple-spot combination were labeled (c), (d), and (e) in Figure 5b. The size of the (e) spot is  $\sim 0.5$  nm, which is similar to that of As(III). The size of the other two spots is  $\sim 0.4$  nm each, which is similar to the size of carbonate. Thus, it is reasonable to conclude that the triple-spot combination consists of one As(III) and two carbonate molecules.

The clear identification of the three spots in the triple-spot-shaped image suggests that the As(III) and carbonate were loosely bonded. Chemical species can be associated through weak and noncovalent interactions, such as hydrogen bonding, electrostatic interactions, electron-donor/electron-acceptor interactions, and  $\pi$ – $\pi$  stacking interactions.<sup>35,36</sup> At circumneutral pH, As(III) exists in neutral  $\text{As}(\text{OH})_3$  species<sup>7</sup> and  $\text{HCO}_3^-$  is the predominant

(34) Guo, X.-C.; Madix, R. J. *Surf. Sci.* **2001**, *489*, 37.

(35) Lehn, J.-M. *Science* **1993**, *260*, 1762.

(36) Dinolfo, P. H.; Hupp, J. T. *Chem. Mater.* **2001**, *13*, 3113.

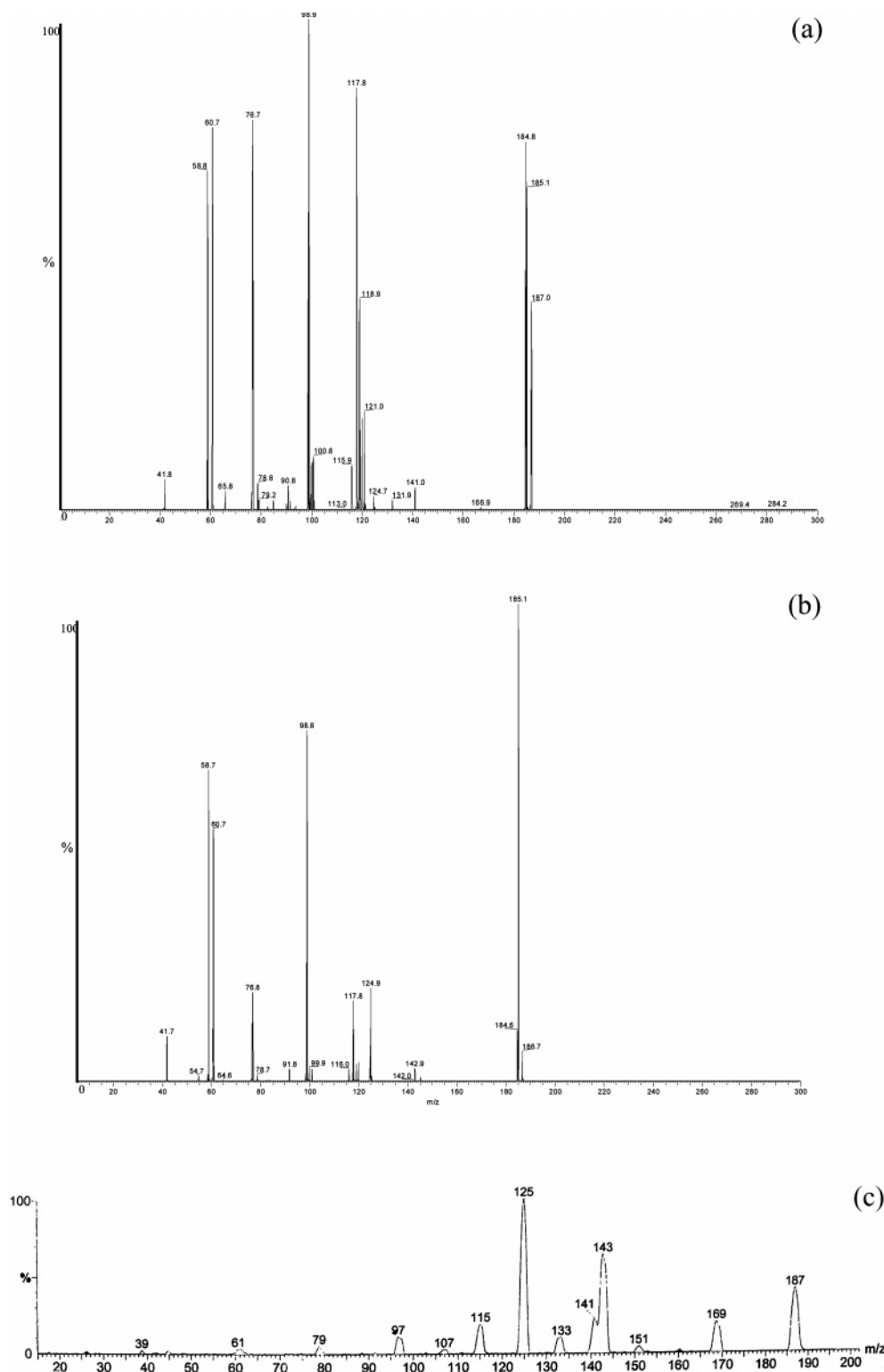


**Figure 9.** MS spectra of the aged As(III)–carbonate solution at different cone voltage (a) 25 and (b) 30 V. (c) MS/MS analysis of the daughter ions of the  $m/z$  187 species.

carbonate species. It is possible that arsenious acid was associated with bicarbonate anions through the formation of H-bonds between the hydroxyl of As(III) and the oxygen of carbonyl group. The tentative molecular model of the  $\text{As}(\text{OH})_3(\text{HCO}_3^-)_2$  complex is also shown in Figure 5d. The STM images in Figure 5b and the models in Figure 5d indicate that each unit consists of an  $\text{As}(\text{OH})_2\text{CO}_3^-$  and an  $\text{As}(\text{OH})_3(\text{HCO}_3^-)_2$ .

The complexes of As(III) and carbonate could be formed in the aged solution and then deposited on the Au(111) surface or could be directly formed on the surface. To determine whether the complexes were formed in the solution, a test was conducted by mixing equal volumes of 0.1 mM As(III) and carbonate solutions and immediately immersing the single-crystal gold bead into the mixed solution for 1 min to deposit the molecules on it.



The electrode was rinsed and imaged with the same procedures as those used for the image of the aged solution. Figure 6 is one of the typical STM images for the fresh As(III)–carbonate solution. No elongated spot or triple-spot-shaped species were observed in the figure. The results indicated that the As(III) and carbonate complexes were formed in the aged solution.

As a comparison to the As(III)–carbonate systems, an investigation of the species in the mixed solution of As(V)–carbonate was also carried out. Panels a and b in Figure 7 show the presence of big and small spots, which formed an ordered adlayer on the Au(111) surface. The spots were marked with red balls and black balls, respectively. Based on the size of the spots, it is deduced that the larger spots are As(V) and the smaller ones are carbonate. The adlayer structure is  $(2\sqrt{3} \times 4\sqrt{3})$  as shown by the drawn unit cell superimposed in Figure 7b. Each unit cell contains one As(V) and three carbonates as indicated in Figure 7b and c. The images showed that no complexes were formed in the mixed solution of As(V) and carbonate under the experimental conditions.

It is interesting to note the mixed distribution of As(V) and carbonate on the Au(111) surface. When both species competed for the surface, the well-ordered networks of carbonates in Figure 4 were replaced by a pattern of alternate double rows of carbonate and a row of As(V). The As(V) anions are separated far from each other in the row, possibly due to the electrostatic repulsion between the anions. As(V) is present predominantly in  $\text{HAsO}_4^{2-}$  species at neutral pH.<sup>7</sup>

**Determination of As(III)–Carbonate Complexes Using IC and ESI-MS/MS.** In order to verify the formation of As(III)–carbonate complexes in the solutions, IC and MS analyses were performed. Figure 8 shows the IC chromatograms obtained for (a) single As(III) solution, (b) aged As(III)–carbonate solution, and (c) fresh As(III)–carbonate solution. A peak at a retention time of 10 min was observed for the single As(III) solution. A similar peak could be seen in the aged and fresh As(III)–carbonate solutions. Lee and Nriagu<sup>10</sup> reported that As(III) had a similar retention time under similar analytical conditions. A distinct peak with an elution time of 19 min was only detected for the aged As(III)–carbonate solution. The new peak at 19 min indicated a As(III)–carbonate species was formed in the aged As(III)–carbonate solution since the retention time of As(V) was 42.5 min (data not shown in the figure). However, the chemical composition of the As(III)–carbonate species cannot be determined by the IC analysis. Lee and Nriagu<sup>10</sup> observed three new peaks with the elution time of 16–25 min in a solution prepared by arsenic trioxide solution saturated with  $\text{CO}_2$  for 24 h. The three peaks were attributed to  $\text{As}(\text{CO}_3)_2^-$ ,  $\text{As}(\text{OH})_2(\text{CO}_3)^-$ , and  $\text{As}(\text{OH})(\text{CO}_3)_2^{2-}$  species without further investigation.

The possible chemical formula of the As(III)–carbonate species in the aged binary component solution was determined using MS. Figure 9a showed the MS spectra of the solution at the cone voltage of 25 V. A new peak appeared at the mass-to-charge ratio ( $m/z$ ) 187, compared to the spectra of single As(III), As(V), and carbonate solutions (the MS spectra of the single-component solutions are not shown here). The  $m/z$  187 peak can be caused by three chemical species in the As(III)–carbonate system, including  $\text{As}(\text{OH})_2\text{CO}_3 \cdot \text{H}_2\text{O}$ ,  $\text{As}(\text{OH})_3 \cdot \text{HCO}_3^-$ , and  $\text{HCO}_3^- \cdot 7\text{H}_2\text{O}$ . These species may be formed in the solution and

in the electrospray ionization process. The cone voltage was changed to check whether the  $m/z$  187 species was composed of As(III). When the cone voltage was increased from 25 V in Figure 9a to 30 V in Figure 9b, the height of the new peak decreased dramatically. At the same time, the amount of  $\text{H}_2\text{AsO}_3^-$  species increased as indicated by the  $m/z$  125 peak (124.7 and 124.9 in Figure 9a and b, respectively). The variation of the  $m/z$  187 and 125 peaks with the cone voltage change suggested that most of the  $m/z$  187 species contained As(III).

MS/MS was used to further verify the chemical formula of the  $m/z$  187 species. The MS/MS spectra in Figure 9c showed the daughter ions of  $m/z$  187 species. The major daughter ions are  $\text{H}_2\text{AsO}_3^-$  ( $m/z$  125),  $\text{H}_2\text{AsO}_3^- \cdot \text{H}_2\text{O}$  (143), and  $\text{As}(\text{OH})_2\text{CO}_3^-$  ( $m/z$  169) or  $\text{HCO}_3^- \cdot 6\text{H}_2\text{O}$  ( $m/z$  169). The smaller peaks can be attributed to  $\text{HCO}_3^- \cdot 5\text{H}_2\text{O}$  ( $m/z$  151),  $\text{H}_2\text{AsO}_4^-$  ( $m/z$  141),  $\text{HCO}_3^- \cdot 4\text{H}_2\text{O}$  ( $m/z$  133),  $\text{HCO}_3^- \cdot 3\text{H}_2\text{O}$  ( $m/z$  115),  $\text{HCO}_3^- \cdot 2\text{H}_2\text{O}$  ( $m/z$  97),  $\text{HCO}_3^- \cdot \text{H}_2\text{O}$  ( $m/z$  79), and  $\text{HCO}_3^-$  ( $m/z$  61). The MS spectroscopic results confirmed the presence of  $\text{As}(\text{OH})_2\text{CO}_3 \cdot \text{H}_2\text{O}$ ,  $\text{As}(\text{OH})_3 \cdot \text{HCO}_3^-$ , or both.

Based on the STM and MS results, As(III) formed complexes with carbonate through As–O–C and hydrogen bonds. The  $\text{As}(\text{OH})_2\text{CO}_3^-$  and  $\text{As}(\text{OH})_2\text{CO}_3^- \cdot \text{H}_2\text{O}$  species determined with STM and MS, respectively, are essentially the same species since ions are usually hydrated in water. The hydrogen bond species include  $\text{As}(\text{OH})_3 \cdot (\text{HCO}_3^-)_2$  (determined by STM) and  $\text{As}(\text{OH})_3 \cdot \text{HCO}_3^-$  (determined by MS). It is possible that one  $\text{HCO}_3^-$  was disassociated from the  $\text{As}(\text{OH})_3 \cdot (\text{HCO}_3^-)_2$  species in the electrospray ionization process since the hydrogen bond is weak. Because only a new IC peak was detected in the aged As(III)–carbonate solution and the As–O–C bond is much stronger than a hydrogen bond, we attributed it to the  $\text{As}(\text{OH})_2\text{CO}_3^-$ . It is possible that the relatively unstable  $\text{As}(\text{OH})_3 \cdot (\text{HCO}_3^-)_2$  species disassociated in the chromatographic separation process in the AS14 anion-exchange column.

## SUMMARY

This study demonstrated that ECSTM is a powerful tool for imaging chemical species and formation of complexes. High-resolution STM images revealed the structural details, molecular arrangements, and interactions between As(III) and carbonate. The STM images showed that As(III) formed complexes with carbonate. A comparison of the images for the aged and freshly mixed solutions of As(III) and carbonate suggested that the complexes were formed in the aged solution, rather than on the Au(111) surface. No complexation was observed between As(V) and carbonate. The formation of the As(III)–carbonate complexes was further confirmed with IC and ESI-MS/MS analyses in the aged solution. Both ECSTM and the mass spectroscopic results determined the formation of  $\text{As}(\text{OH})_2\text{CO}_3^-$  species. As(III) and carbonate also formed an unstable complex through a hydrogen bond.

Received for review November 27, 2006. Accepted March 19, 2007.

AC062244T